

Transmission electron microscopy of $\text{SrAl}_2\text{Si}_2\text{O}_8$: Feldspar and hexacelsian polymorphs

JUTTA TÖPEL-SCHADT

Institut für Kristallographie und Mineralogie, Johann Wolfgang Goethe-Universität, D-6000 Frankfurt/M., Germany

W. F. MÜLLER

Fachbereich 11, Mineralogie, Technische Hochschule Darmstadt, D-6100 Darmstadt, Germany

H. PENTINGHAUS

Institut für Mineralogie, Westf. Wilhelms-Universität, D-4400 Münster/Westf., Germany

Sr-feldspar: The electron diffraction data obtained agree with the space group $I2/c$ determined by X-ray methods. The antiphase domains present are considered to originate from a subsolidus phase transition due to ordering of Al and Si. Polysynthetic twins of the Carlsbad law have been found. Sr-hexacelsian: Three polymorphs with the probable space groups $P6/mmm$, $P6_3/mcm$ and $Immm$ have been observed, the latter two for the first time in this compound. Both $P6/mmm$ and $P6_3/mcm$ polymorphs were present at room temperature. When heated above $\sim 600^\circ\text{C}$, the $P6_3/mcm$ polymorph transforms rapidly and reversibly to the pseudohexagonal orthorhombic phase with the space group $Immm$. $P6_3/mcm$ -Sr-hexacelsian shows antiphase domains with the displacement vector $\frac{1}{2}c$ and $Immm$ -Sr-hexacelsian contains twin domains with the three-fold twin axis parallel to c . The occurrence of antiphase and twin domains, respectively, agrees with the symmetry reductions involved with the phase transitions. This is shown by aid of the group–subgroup relationships among the space groups $P6/mmm$, $P6_3/mcm$ and $Immm$.

1. Introduction

The alkaline earth aluminum silicates $\text{CaAl}_2\text{Si}_2\text{O}_8$, $\text{SrAl}_2\text{Si}_2\text{O}_8$ and $\text{BaAl}_2\text{Si}_2\text{O}_8$ are important constituents of phase systems of high interest in nature and ceramics. For example, the plagioclase feldspar series $\text{Na}_x\text{Ca}_{1-x}\text{Al}_{2-x}\text{Si}_{2+x}\text{O}_8$ ($0 \leq x \leq 1$) are the most common minerals of the earth's crust and have been the topic of numerous studies [1]. Polymorphs of $\text{BaAl}_2\text{Si}_2\text{O}_8$ frequently occur in optical glasses, in ceramic and glass-ceramic products [2]. The present study by means of transmission electron microscopy (TEM) is intended to contribute to the knowledge of polymorphism and crystal defects of $\text{SrAl}_2\text{Si}_2\text{O}_8$ which is the least investigated compound of those mentioned above.

The polymorphs so far known of $\text{SrAl}_2\text{Si}_2\text{O}_8$ crystallize in the structures of feldspar, paracelsian, and hexacelsian. The Sr-feldspar is the stable phase between about 500°C and the melting point at 1650°C , Sr-paracelsian is stable from room temperature up to 500°C , and Sr-hexacelsian which is metastable in the whole temperature range can only be prepared by quenching of a superheated melt. The feldspar and hexacelsian polymorphs of $\text{SrAl}_2\text{Si}_2\text{O}_8$ are only known as synthetic products. Sr-paracelsian, however, has just been reported to occur as a mineral called slawsonite [3].

Bruno and Gazzoni [4] found that the space group of ordered Sr-feldspar is $I2/c$; a crystal structure refinement was done by Chiari *et al.* [5]. Sr-feldspar and celsian ($\text{BaAl}_2\text{Si}_2\text{O}_8$) are iso-

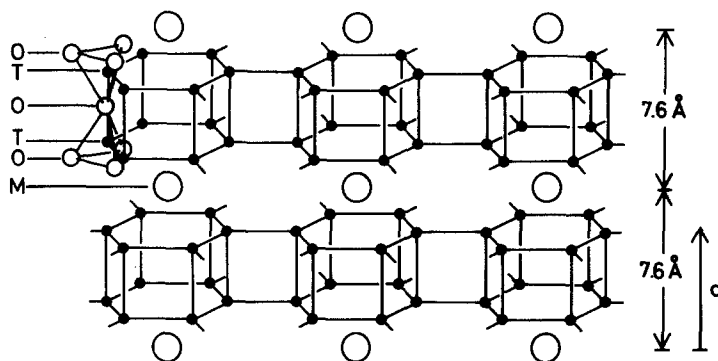


Figure 1 Hexacelsian structure with the characteristic double-tetrahedra sheets. M:Ca, Sr, Ba, Pb; T:Si, Al, Ge; O: oxygen, $c = 7.6 \text{ \AA}$ for Sr-hexacelsian with the space group P6/mmm.

structural. No X-ray single crystal data of Sr-hexacelsian are available at present. X-ray powder data have been published by Sorrell [6], Barrer and Marshall [7], and Sirazhiddinor [8, 9]. All authors based their indexing on an hexagonal cell with $c \sim 7.6 \text{ \AA}$. Hexacelsian – originally the name of an hexagonal polymorph of $\text{BaAl}_2\text{Si}_2\text{O}_8$ – now denotes a structure family. Known end-members crystallizing in the hexacelsian structure are $\text{RbAlSi}_3\text{O}_8$, $\text{CaAl}_2\text{Si}_2\text{O}_8$, $\text{SrAl}_2\text{Si}_2\text{O}_8$, $\text{BaAl}_2\text{Si}_2\text{O}_8$, $\text{PbAl}_2\text{Si}_2\text{O}_8$, and $\text{BaAl}_2\text{Ge}_2\text{O}_8$ [10, 11]. In the basic hexacelsian structure (Al, Si) O_4 -tetrahedra share three corners in a way which yields an hexagonal sheet with the remaining apices pointing into the same direction, cf. Fig. 1. Two of those sheets join through sharing of their apical oxygens thus forming a double tetrahedra sheet. The large cations lie between such double sheets. The sheet symmetry is hexagonal or pseudohexagonal.

Systematic work on crystal defects in Sr-feldspar has not been published so far. Only Bruno and Gazzoni [4] described Carlsbad twins in their sample and Müller [12] observed antiphase domains in a non-stoichiometric sample by means of TEM. Even less is known on Sr-hexacelsian. As mentioned above, no X-ray single crystal data exist and the space group(s) of Sr-hexacelsian are not known. There are no informations on presence and nature of crystal defects in Sr-hexacelsian.

TEM methods including electron diffraction, bright-field, dark-field, and lattice imaging were used in order to study crystal defects and to determine the space groups of Sr-feldspar and Sr-hexacelsian. The purpose of this study was also to reveal similarities and differences between the corresponding polymorphs $\text{SrAl}_2\text{Si}_2\text{O}_8$, $\text{CaAl}_2\text{Si}_2\text{O}_8$, and $\text{BaAl}_2\text{Si}_2\text{O}_8$ regarding crystal structure, phase transitions and crystal defects.

2. Materials and techniques

The Sr-feldspar was prepared by slow cooling of a stoichiometric melt. Its lattice parameters determined by X-ray Guinier powder patterns are:

$$\begin{aligned} a &= 8.3923 (7) \text{ \AA} \\ b &= 12.9708 (8) \text{ \AA} \\ c &= 14.2681 (12) \text{ \AA} \\ \beta &= 115.451 (5) (^\circ). \end{aligned}$$

The Sr-hexacelsian could only be obtained by quenching a superheated melt (1700°C) to room temperature. The lattice parameters based on hexagonal indexing are:

$$\begin{aligned} a &= 5.1931 (15) \text{ \AA} \\ c &= 7.5963 (23) \text{ \AA}. \end{aligned}$$

Suitable thin specimens for TEM with 100 kV acceleration voltage were prepared from conventional petrographic thin sections by ion bombardment [13–15]. Specific conditions are described by Müller and Wenk [16]. TEM observations were made with the aid of a JEOL JEM 100B electron microscope equipped with a side entry goniometer. In order to observe possible phase transitions at elevated temperatures *in situ* a commercially available heating holder was used. The TEM methods employed in this study for analysing crystal defects are described in textbooks in detail [17–19].

3. Sr-feldspar: Observations and results

3.1. Antiphase domains

Selected area electron diffraction patterns of single crystals which commonly had a size of about 5 to $50 \mu\text{m}$ were in agreement with the space group I2/c [4]: only reflections with $h + k = 2n, l = 2n$ (type “a”) and with $h + k = 2n + 1, l = 2n + 1$ (type “b”) were found. Reflections of the kind $h + k = 2n, l = 2n + 1$ and $h + k = 2n + 1, l = 2n$ have not been seen, cf. Fig. 2a (both types of reflec-

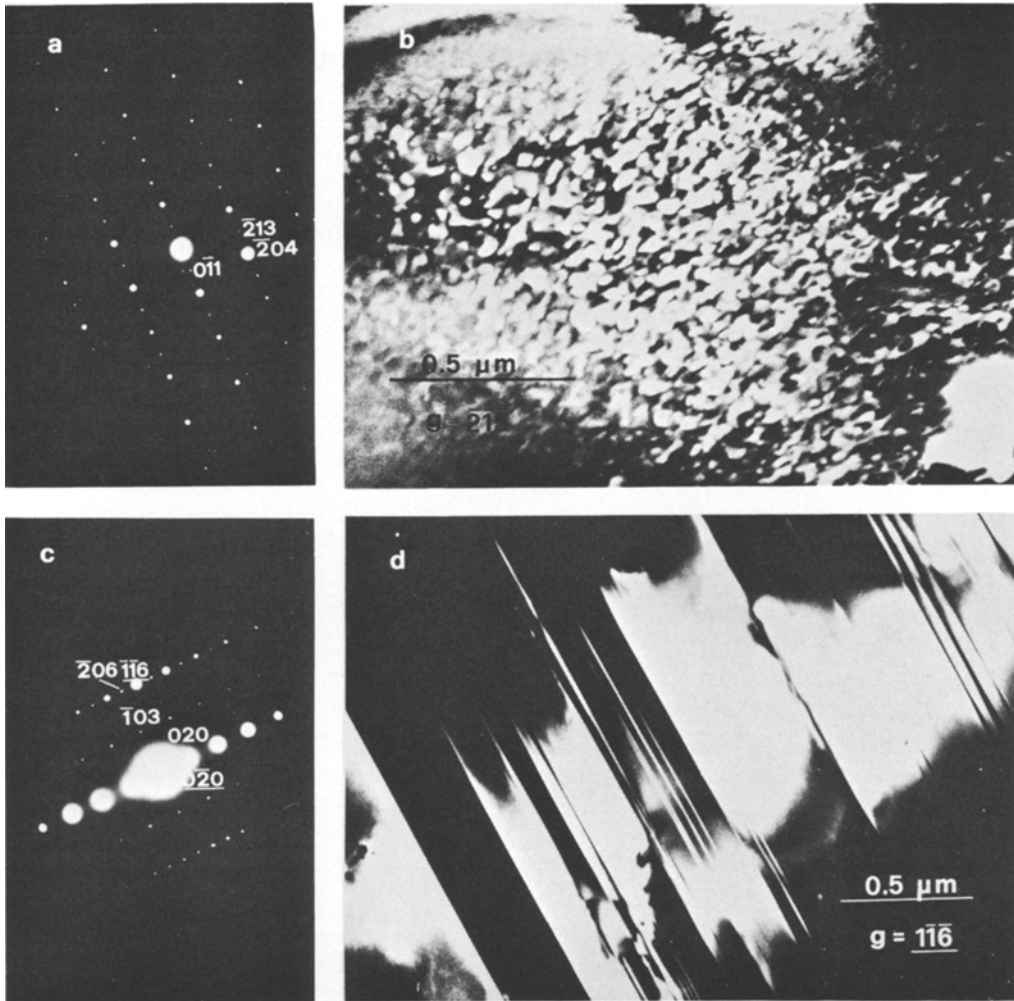


Figure 2 Sr-feldspar. (a) Typical electron diffraction pattern displaying reflections of the type “a” ($h + k = 2n, l = 2n$) and type “b” ($h + k = 2n + 1, l = 2n + 1$). (b) Antiphase domains. TEM dark-field image with $g = \underline{215}$. (c) Diffraction pattern of a crystal twinned according to the Carlsbad law (twin axis parallel c); twin reflections are underlined. (d) Carlsbad twins. The composition plane is parallel to (010) . TEM dark-field image with $g = \underline{116}$.

tions occur also in anorthite, the Ca-feldspar, $\text{CaAl}_2\text{Si}_2\text{O}_8$). Dark-field images using b-reflections revealed antiphase domains about 500 to 1000 Å in size (Fig. 2b). They were out of contrast with a-reflections operating. According to the visibility–invisibility criteria, the displacement vector of the antiphase domains is $1/2c$ (cf. textbooks mentioned above; a recent discussion of TEM of domains has been given by Amelinckx and Van Landuyt [18]).

3.2. Twins

The crystals commonly display polysynthetic twinning of the Carlsbad law, i.e. 180° rotation

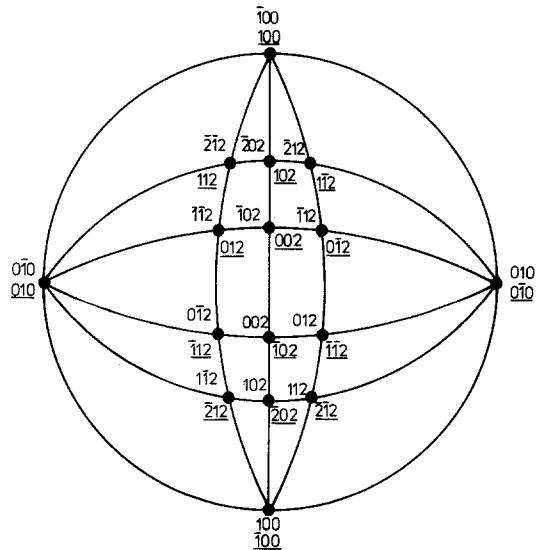


Figure 3 Stereographic projection of Sr-feldspar. The indices of the planes in twin orientation are underlined.

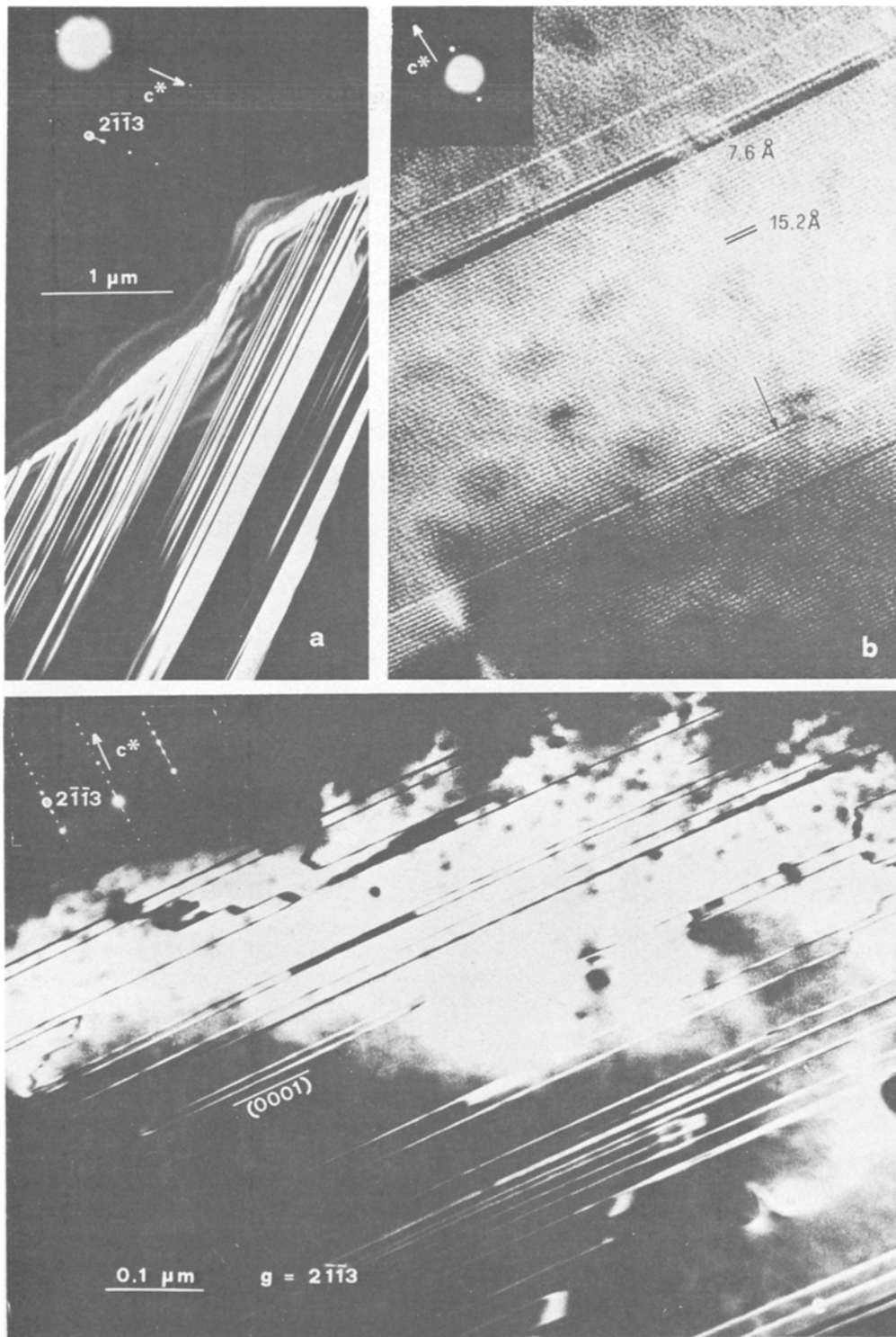


Figure 4 Sr-hexacelsian. (a) Lamellar intergrowth parallel to (001) of P6₃/mmm- and P6₃/mcm-Sr-hexacelsian. Lamellae of P6₃/mcm-Sr-hexacelsian are bright. TEM dark field image with $g = 2\bar{1}\bar{1}3$ which is a reflection only of the P6₃/mcm-Sr-hexacelsian. The corresponding electron diffraction pattern is inserted. (b) Lattice image of (001) planes of P6₃/mcm phase with $c \sim 15.2 \text{ \AA}$ and P6/mmm with $c \sim 7.6 \text{ \AA}$ (easily seen on the original photograph). An antiphase domain boundary (APB) in P6₃/mcm-Sr-hexacelsian is indicated by an arrow. (c) APBs in P6₃/mcm-Sr-hexacelsian. TEM dark-field image with $g = 2\bar{1}\bar{1}3$.

about c . The twin lamellae have (010) as composition plane and are sometimes only a few unit cells in width. Due to the special lattice metric of Sr-feldspar which was already discussed by Bruno and Gazzoni [4] the twin reflections appear at the positions of type d -reflections ($h + k = 2n + 1$, $l = 2n$) cf. Fig. 2c. Dark-field images with these reflections operating proved that they were indeed twin reflections (cf. Fig. 2d). Fig. 3 displays the stereographic projection of Sr-feldspar, indices of the planes in twin orientation are underlined.

4. Sr-hexacelsian: Observations and results

4.1. Phases present at room temperature

At room temperature, two hexagonal Sr-hexacelsian polymorphs occur in the sample; one has the lattice parameter $c \sim 7.6 \text{ \AA}$, the other has $c \sim 2 \times 7.6 \text{ \AA} \sim 15.2 \text{ \AA}$. The two polymorphs occur as oriented intergrowth with a and c parallel (cf. Fig. 4a). Their common composition plane is (001), which is the plane of the $\text{Al}_2\text{Si}_2\text{O}_8$ sheets. Electron diffraction patterns of several crystals have been collected in order to determine unit cell data and extinction rules. This was greatly facilitated by the $\pm 60^\circ$ tilt and $\pm 180^\circ$ rotation capabilities of the specimen holder, which helped to obtain many diagnostic orientations of one crystal. In view of the topological features of the hexacelsian structure, the probable space group of the Sr-hexacelsian with $c \sim 7.6 \text{ \AA}$ is $P6/mmm$, that of the polymorph with $c \sim 15.2 \text{ \AA}$ is $P6_3/mcm$. The c glide plane of $P6_3/mcm$ was deduced from systematic absences in the $00l-h\bar{h}0$ diffraction patterns where reflections of the type $h\bar{h}l$ only showed up for l even. Of course, it has to be deter-

mined by careful X-ray single crystal studies, if these space groups are indeed the true ones. In the following, the polymorphs of $\text{SrAl}_2\text{Si}_2\text{O}_8$ -hexacelsian are simply characterized by their space groups and called $P6/mmm$ -Sr-hexacelsian and $P6_3/mcm$ -Sr-hexacelsian, respectively.

It may be mentioned that in addition to the crystalline phases small glassy areas occurred which were about $1 \mu\text{m}$ in size. Qualitative energy dispersive X-ray microanalysis showed that the glass has an higher Si/Al ratio than the Sr-hexacelsian. No differences in chemical composition between the two crystalline polymorphs have been detected.

4.2. Antiphase domain boundaries (APBs) in $P6_3/mcm$ -Sr-hexacelsian

$P6_3/mcm$ -Sr-hexacelsian commonly displays planar lattice defects predominantly oriented parallel to (001), cf. Figs. 4b and c. They were in contrast with reflections of the type hkl with $l = 2n + 1$ and out of contrast with reflections of the type hkl with $l = 2n$. These faults are interpreted as APBs; their displacement vector is $1/2 c$.

4.3. Phase transition $P6_3/mcm \rightleftharpoons Immm$ -Sr-hexacelsian

Controlled heating experiments using the commercial heating holder were performed with a Sr-hexacelsian specimen inside the electron microscope. It turned out that the $P6_3/mcm$ -Sr-hexacelsian undergoes a rapid and reversible phase transition at elevated temperatures. This transition can easily be followed up in the electron diffraction

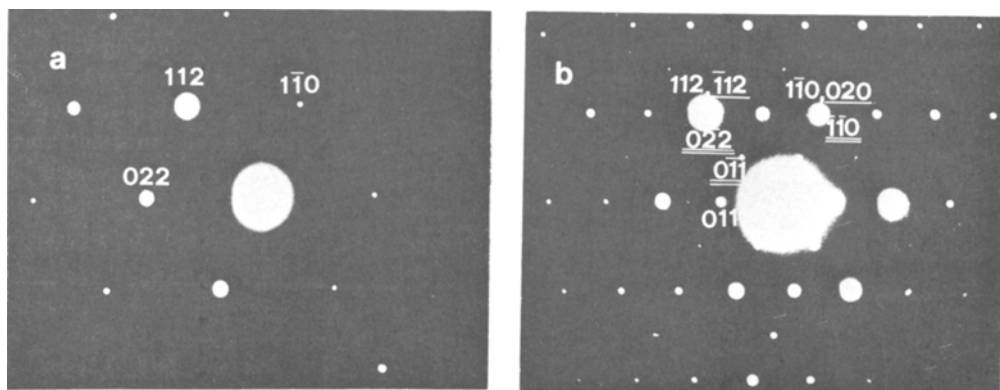


Figure 5 Heating experiment with Sr-hexacelsian. (a) Diffraction pattern of $P6_3/mcm$ -Sr-hexacelsian at room temperature. (b) Diffraction pattern of the same crystal after the phase transition $P6_3/mcm \rightleftharpoons Immm$ at a temperature $\geq 600^\circ \text{ C}$; additional reflections appear, reflections caused by twinning are underlined and the three-fold twin axis lies parallel to c . The reflection between 000 and $\bar{1}10$ was produced by multiple diffraction.

mode because reflections of the type $h + k = 2n$, $l = 2n + 1$ disappear and new reflections of the type $h + k = 2n + 1$, $l = 2n + 1$ become visible (all reflections are given here in the orthorhombic setting), cf. Fig. 5. The new phase has the lattice parameters $a \sim 5.2 \text{ \AA}$, $b \sim 9.0 \text{ \AA}$ and $c \sim 15.2 \text{ \AA}$ and the probable space group *Immm*. The *Immm*-Sr-hexacelsian crystals are commonly fragmented into twin domains. Analysis of the electron diffraction patterns revealed that three orientation variants of twin domains occur; the three-fold axis is parallel to c .

Although the furnace temperature of the heating holder is obtained accurately, the exact temperature of the phase transition cannot be given since it is not measured at the specimen area under observation. The phase transition occurred at furnace temperatures between 700 and 900°C. The reversion back to *P6₃/mcm*-Sr-hexacelsian of the same crystal sometimes took place at a temperature of up to 100°C lower. It is not clear if this is a true hysteresis or an experimental effect due to changes in thermal contact between heater and specimen. In any case, the *Immm* polymorph could not be quenched to room temperature. It may be noted that the polymorph *P6/mmm*-Sr-hexacelsian did not show any structural change in the temperature range up to $\sim 950^\circ \text{C}$ furnace temperature.

4.4. Space group relationships and the occurrence of twin and antiphase domains

Many studies in the field of materials science and mineralogy have shown that the occurrence of twin and antiphase domains is frequently a consequence of order-disorder or displacive phase transitions. The symmetry relations of the domains, e.g. the twin law or the displacement vector of the antiphase domains, allow conclusions to be made regarding the structure of the parent phase which is usually the high temperature phase. Group-theoretical considerations help to understand or to predict the occurrence of domains associated with phase transitions, at least from a geometric point of view [20–24]. Inspection of the tables “Maximal subgroups of the space groups” [25] shows that the space groups *P6/mmm*, *P6₃/mcm* and *Immm* of the polymorphs of Sr-hexacelsian are related to each other as seen in Fig. 6 (adopted from Müller [26]). *P6₃/mcm* and *Immm* are both subgroups of *P6/mmm*, but lie on different

branches of the “family tree” [21]. No twin domains can occur in *P6₃/mcm*-Sr-hexacelsian since it is a (maximal) klassengleiche subgroup of the parent space group *P6/mmm*. But APBs with $1/2 c$ as displacement vector are to be expected and have actually been observed, because *P6₃/mcm* has lost the translational symmetry operation $1/2 c$. *Immm* has lost point group and translational symmetry operations, namely the three-fold axis parallel to c and the translational symmetry operation $1/2 c$. Three orientation variants with the three-fold twin axis parallel to c and antiphase domains with the displacement vector $1/2 c$ are possible in *Immm*-Sr-hexacelsian. Only the twin domains have been found. APBs may also occur but have not been seen so far, possibly because the imaging conditions at the high temperatures were not suitable.

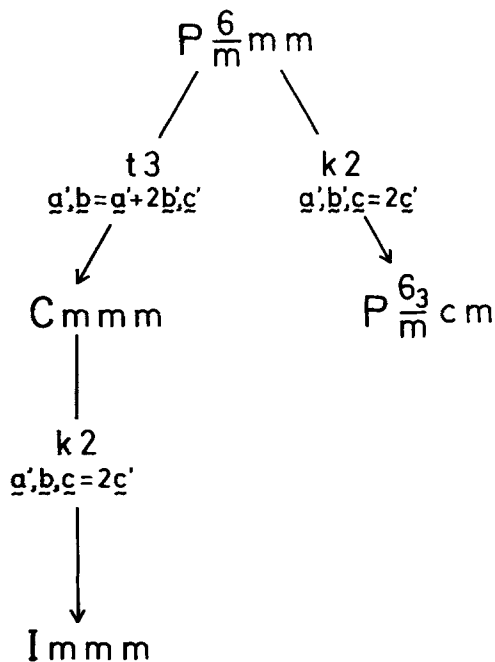


Figure 6 (After [26]). Group-subgroup relationships between the three Sr-hexacelsian modifications with the space groups *P6/mmm*, *P6₃/mcm* and *Immm* observed, displayed in a “family tree”. The unit cell transformations are given in terms of the basic vectors a' , b' and c' of the unit cell of *P6/mmm*. The symmetry-reducing step is symbolized by an arrow which connects a space group with its maximal subgroup. The letters *t* or *k* indicate that the subgroups have the same translational or point group symmetry, respectively, as the corresponding space group. The numbers give the indices of reduction, e.g. *t3* means that the subgroup has the same translational symmetry as the (parent) space group but has lost the point group symmetry of a three-fold axis. Formalism after [21].

5. Discussion

The antiphase domains of Sr-feldspar probably originate from a subsolidus phase transition due to ordering of Al/Si, i.e. each Al tetrahedron is surrounded by Si tetrahedra and vice versa [27]. This is concluded from the fact that the displacement vector $1/2c$ relates sub-lattices of similar atomic coordinates but exactly reversed Al/Si-arrangements. The same type of antiphase domains attributed to the ordering of Al/Si has also been observed in synthetic celsian, $\text{BaAl}_2\text{Si}_2\text{O}_8$, [26] and in natural and synthetic anorthites, $\text{CaAl}_2\text{Si}_2\text{O}_8$, which crystallized from the melt or were obtained by crystallization of glass [28–31]. The displacement vector of the antiphase domains is $1/2c$ for celsian (space group $I2/c$) and $1/2(a+b)$ for anorthite (space group $P\bar{1}$) [29]. The vector $1/2(a+b)$ also relates sublattices with exactly reversed Al/Si-distribution; in a truly body-centred structure $1/2(a+b)$ and $1/2c$ are symmetrically equivalent. It is not yet clear why in anorthite the displacement vector of the antiphase domains is $1/2(a+b)$ and not $1/2c$.

Three Sr-hexacelsian polymorphs have been observed in this study: Their probable space groups are $P6/mmm$, $P6_3/mcm$ and $Immm$. The space group relationships shown in Fig. 6 are identical with those of Ba-hexacelsian (Fig. 4 in [26]). However, in the case of Ba-hexacelsian only the polymorphs $P6_3/mcm$ and $Immm$ have been obtained and identified unequivocally [26]. It is assumed that at very high temperatures ($> 1570^\circ\text{C}$ up to the melting point at $\sim 1760^\circ\text{C}$) a Ba-hexacelsian with the space group $P6/mmm$ is stable, but this has not yet been proven by diffraction methods. Takéuchi and Donnay [32] have shown that hexagonal $\text{CaAl}_2\text{Si}_2\text{O}_8$ has the space group $P6_3/mcm$ and found evidence for mistakes in the stacking sequence of the $\text{Al}_2\text{Si}_2\text{O}_8$ sheets, but no TEM study has been published on this compound so far. If we compare the TEM results on Sr- and Ba-hexacelsian, we recognize close similarities. Both $P6_3/mcm$ polymorphs display the same type of APBs and both change rapidly and reversibly to a pseudo-hexagonal orthorhombic phase with the probable space group $Immm$ which shows twin domains with the three-fold twin axis parallel to c . In $Immm$ -Ba-hexacelsian, ABPs with the displacement vector $1/2c$ have been observed which were not seen in $Immm$ -Sr-hexacelsian, possibly because of experimental difficulties. It is concluded that the phase transition of Sr-hexa-

celsian detected by means of differential thermal analysis and thermal expansion measurements at about 600°C [11, 33] is identical with the phase transition $P6_3/mcm \rightleftharpoons Immm$ reported in this paper. The transition temperature is about 300°C higher than that of the analogous transition in Ba-hexacelsian. Somewhat surprising is the observation that $P6_3/mcm$ -Sr-hexacelsian and the presumable high temperature phase $P6/mmm$ -Sr-hexacelsian both were present at room temperature. A difference in chemical composition of these two phases was not detected. A speculative explanation could be that the Al/Si long-range order in Sr-hexacelsian was only partially completed at high temperatures due to the rapid quenching of the melt. When cooled down, only those areas with Al/Si order underwent the transitions to $Immm$ and $P6_3/mcm$ while the Sr-hexacelsian with disordered Al/Si distribution retained the space group $P6/mmm$.

Acknowledgements

We thank Professor M. Korekawa for helpful discussions and encouraging interest in this work and A. Haake, M. Spahn and K. Hess for technical assistance. Support by the Deutsche Forschungsgemeinschaft is gratefully acknowledged.

References

1. J. V. SMITH, "Feldspar Minerals", Vol. 1 (Springer-Verlag, Berlin, Heidelberg, New York, 1974).
2. G. OEHLISCHLEGEL, K. ABRAHAM and O. W. FLÖRKE, *Krist. und Techn.* **11** (1976) 59.
3. D. T. GRIFFIN, P. H. RIBBE and G. V. GIBBS, *Amer. Mineral.* **62** (1977) 31.
4. E. BRUNO and G. GAZZONI, *Z. Krist.* **132** (1970) 327.
5. G. CHIARY, M. CALLERI, E. BRUNO and P. RIBBE, *Amer. Mineral.* **60** (1975) 111.
6. C. A. SORRELL, *Amer. Mineral.* **47** (1962) 291.
7. R. M. BARRER and D. J. MARSHALL, *J. Chem. Soc.* **1** (1964) 485.
8. N. A. SIRAZHIDDINOV, P. A. ARIFOV and R. G. GREBENSHCHIKOV, *Izv. Akad. Nauk. SSSR, Neorg. Mater* **7** (1971) 1581.
9. *Idem, ibid.* **8** (1972) 870.
10. H. PENTINGHAUS, *Fortschr. Mineral.* **53** Beih. **1** (1975) 65.
11. *Idem*, Habilitationsschrift (1978) (in preparation).
12. W. F. MÜLLER, Proceedings of the 8th International Congress on Electron Microscopy, Canberra, Vol. 1 (1974) 472.
13. H. BACH, *Bosch Techn. Berichte* **1** (1964) 10.
14. D. J. BARBER, *J. Mater. Sci.* **5** (1970) 1.
15. N. TIGHE, "Electron Microscopy in Mineralogy", edited by H.-R. Wenk (Springer-Verlag, Heidelberg, New York, 1976) p. 144.

16. W. F. MÜLLER and H.-R. WENK, *N. Jb. Miner. Mh.* **H1** (1973) 17.
17. P. B. HIRSCH, A. HOWIE, R. B. NICHOLSON, D. W. PASHLEY and M. J. WHELAN, "Electron Microscopy of Thin Crystals" (Butterworths, London, 1965).
18. S. AMELINCKX, R. GEVERS, G. REMAUT and J. VAN LANDUYT (editors) "Modern Diffraction and Imaging Techniques in Materials Science" (North Holland Press, Amsterdam, 1970).
19. H.-R. WENK (coordinating editor, "Electron Microscopy in Mineralogy" (Springer-Verlag, Berlin, Heidelberg, New York, 1976).
20. S. AMELICKX and J. VAN LANDUYT, "Electron Microscopy in Mineralogy", edited by H.-R. Wenk (Springer-Verlag, Berlin, Heidelberg, New York, 1976) p. 68.
21. H. BÄRNIGHAUSEN, *Acta Cryst.* **A31** (1975) 3.
22. *Idem*, private communication (1975).
23. G. VAN TENDELOO and S. AMELINCKX, *Acta Cryst.* **A 30** (1975) 431.
24. J. WONDRAATSCHEK and W. JEITSCHKO, *ibid.* **A 32** (1976) 664.
25. J. NEUBÜSER and H. WONDRAATSCHEK, private communication (1969) (to be published in International Tables of Crystallography).
26. W. F. MÜLLER, *Phys. Chem. Minerals* **1** (1977) 71.
27. F. LAVES and J. R. GOLDSMITH, *Z. Krist.* **106** (1955) 227.
28. J. M. CHRISTIE, J. S. LALLY, A. H. HEUER, R. M. FISHER, D. T. GRIGGS and S. V. RADCLIFF, Proceedings of the 2nd Lunar Scientific Conference, *Geochim. Cosmochim. Acta. Suppl.* **2 Vol. 1** (1971) p. 69.
29. W. F. MÜLLER, H.-R. WENK, N. L. BELL and G. THOMAS, *Contr. Mineral. and Petrol.* **40** (1973) 63.
30. A. C. McLAREN and D. B. MARSHALL, *ibid.* **44** (1974) 237.
31. H. KROLL and W. F. MÜLLER, *Fortschr. Mineral.* **55** Beih. 1 (1977) 77.
32. Y. TAKEUCHI and DONNAY, *Acta Cryst.* **12** (1956) 465.
33. D. BAHAT, *J. Mater. Sci.* **7** (1972) 198.

Received 14 November and accepted 19 December 1977.